AIP Journal of Applied Physics

# Structure and optically pumped lasing from nanocrystalline ZnO thin films prepared by thermal oxidation of ZnS thin films

X. T. Zhang, Y. C. Liu, L. G. Zhang, J. Y. Zhang, Y. M. Lu et al.

Citation: J. Appl. Phys. **92**, 3293 (2002); doi: 10.1063/1.1498958
View online: http://dx.doi.org/10.1063/1.1498958
View Table of Contents: http://jap.aip.org/resource/1/JAPIAU/v92/i6
Published by the American Institute of Physics.

## Related Articles

The effect of interfaces on magnetic activation volumes in single crystal Co2FeSi Heusler alloy thin films
Appl. Phys. Lett. 101, 102410 (2012)

Composition, nanostructure, and optical properties of silver and silver-copper lusters
J. Appl. Phys. 112, 054307 (2012)

Independent wavelength and density control of uniform GaAs/AlGaAs quantum dots grown by infilling self-assembled nanoholes
J. Appl. Phys. 112, 054303 (2012)

Effect of photodiode angular response on surface plasmon resonance measurements in the Kretschmann-Raether configuration
Rev. Sci. Instrum. 83, 093102 (2012)

Structural and dielectric properties of poly(vinylidene fluoride)–based terpolymer/copolymer blends developed on aluminum foil
J. Appl. Phys. 112, 053505 (2012)

## Additional information on J. Appl. Phys.

Journal Homepage: http://jap.aip.org/
Journal Information: http://jap.aip.org/about/about_the_journal
Top downloads: http://jap.aip.org/features/most_downloaded
Information for Authors: http://jap.aip.org/authors

ADVERTISEMENT

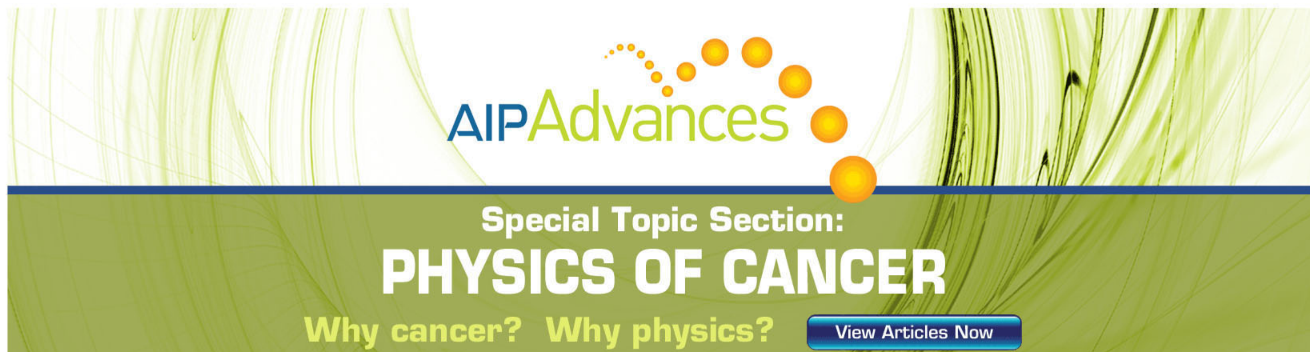


Downloaded 09 Sep 2012 to 159.226.165.151. Redistribution subject to AIP license or copyright; see http://jap.aip.org/about/rights_and_permissions

# Structure and optically pumped lasing from nanocrystalline ZnO thin films prepared by thermal oxidation of ZnS thin films

X. T. Zhang, Y. C. Liu,[a] L. G. Zhang, J. Y. Zhang, Y. M. Lu, D. Z. Shen, W. Xu, G. Z. Zhong, X. W. Fan, and X. G. Kong
*Open Laboratory of Excited State Processes, Chinese Academy of Sciences, Changchun Institute of Optics, Fine Mechanics and Physics, Chinese Academy of Sciences, 1- Yan An Road, Changchun, 130021, People's Republic of China*

(Received 1 October 2001; accepted for publication 11 June 2002)

In this article, we observe the optically pumped lasing from the high-quality nanocrystalline ZnO thin films obtained by thermal oxidation of ZnS thin films, which were grown on $SiO_2$ substrates by low-pressure-metalorganic chemical vapor deposition technique. The x-ray diffraction (XRD) patterns indicate that high-quality ZnS films possess a preferred (111) orientation. ZnS has a transformation to ZnO at an annealing temperature ($T_a$) of 500 °C, and fully transforms into ZnO at $T_a \geqslant 700$ °C from the XRD patterns. The obtained ZnO films possess a polycrystalline hexagonal wurtzite structure. The fifth-order Raman scattering is observed in the films, which indicates that a large deformation energy exists in the lattice. In photoluminescence (PL), spectra, for all the samples with different annealing temperatures, the near-band-edge (NBE) PL peak has a pronounced blueshift with increasing annealing temperature, while the full width at half maximum (FWHM) decreases gradually. We think that emissions of the bound excitons play an important role in NBE PL. A strong PL with a FWHM of 62 meV at 3.30 eV from NBE has been obtained at room temperature for the samples annealed at 900 °C. The PL intensity ratio of the ultraviolet emission to the deep-level emission is as high as 98 at room temperature, indicating the high-quality of the nanocrystalline ZnO films. © *2002 American Institute of Physics.* [DOI: 10.1063/1.1498958]

## I. INTRODUCTION

Zinc oxide (ZnO) is an interesting wide band gap semiconductor material with a direct band gap of 3.37 eV at room temperature. It makes more attention to the ultraviolet (UV) optoelectronic devices, such as UV laser, optical waveguide, and exciton-related devices.[1–3] To produce these devices, many techniques have been used to prepare ZnO thin films, for example, rf magnetron sputtering,[4] metalorganic chemical vapor deposition (MOCVD),[5] molecular-beam epitaxy (MBE),[6,7] pulsed laser deposition,[8] and reactive thermal evaporation.[9] The photoluminescence (PL) spectra of ZnO thin films show a near band edge (NBE) UV emission and a defect-related deep-level (DL) emission which precludes various applications, such as UV luminescence devices. The DL emissions are usually related to structural defects and impurities. All structural defects originate from an insufficient supply of oxygen during growth. In order to overcome these difficulties and obtain a strong UV NBE emission and a much weaker emission band correlated with DL defects, it is necessary to prepare a high-quality ZnO thin film.

As is well known, it is difficult to directly prepare high-quality ZnO thin film by the MOCVD technique. This is because oxygen ($O_2$) used in the experiment easily oxidizes the organic source. Furthermore, it is a puzzling problem to accurately control the flow rate of the oxygen ($O_2$). However, high-quality ZnS films are easily grown on quartz substrate by the MOCVD technique. In addition, the ZnS compound can be very easily oxidized to form ZnO and $SO_2$. For ZnO used in optoelectronic devices, to prepare high-quality thin films is necessary. Up until now, the most high-quality ZnO thin films with an intense UV luminescence or the stimulated emission are to be grown on sapphire substrates by different growth techniques.[10,11] Assuming that ZnO thin films grown on $SiO_2$ substrates have a perfect crystal structure with a good luminescence performance, compared with ZnO thin films grown on sapphire substrates, there could be many advantages in luminescence devices. One of the advantages is that the ZnO samples used in our experiments form a dielectric planar waveguide structure consisting of a thin ZnO ($n=2.45$) layer surrounded by air ($n=1$) on one side and $SiO_2$ ($n=1.46$) on the other. This should be beneficial to confine light divergence from ZnO layers. In this article, we present a useful and simple method for preparing nanocrystalline ZnO thin films with good UV luminescent performance, that is thermal oxidation of ZnS films on $SiO_2$ substrates grown by the low-pressure-metalorganic chemical vapor deposition (LP-MOCVD) technique.

## II. EXPERIMENTS

The ZnS thin films were grown on quartz substrates using dimethyl zinc (DMZn) and hydrogen sulfide ($H_2S$) by the low-pressure-metalorganic chemical vapor deposition (LP-MOCVD) technique. The gas flow rates of DMZn and $H_2S$ were fixed at $28.65\times10^{-6}$ mol/min and $4.00\times10^{-4}$ mol/min, respectively. Hydrogen ($H_2$) was used as the carrier gas

[a]Also at: Institute of Theoretical Physics, Northeast Normal University, Changchun 130024, People's Republic of China; author to whom all correspondence should be addressed; electronic mail: liuyichun@mail.china.com

 © 2002 American Institute of Physics

Downloaded 09 Sep 2012 to 159.226.165.151. Redistribution subject to AIP license or copyright; see http://jap.aip.org/about/rights_and_permissions

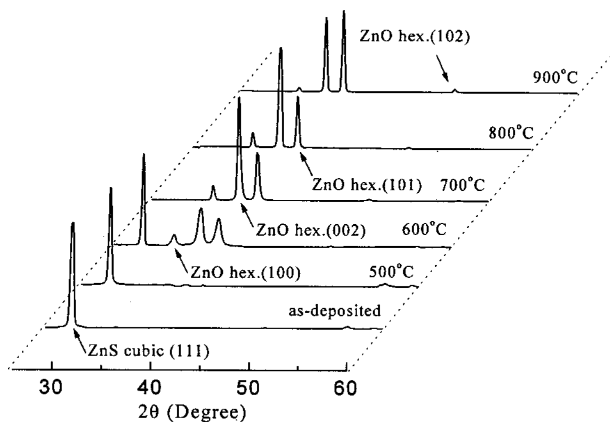


FIG. 1. The XRD patterns of the ZnO thin films at different annealing temperatures and as-deposited ZnS sample.

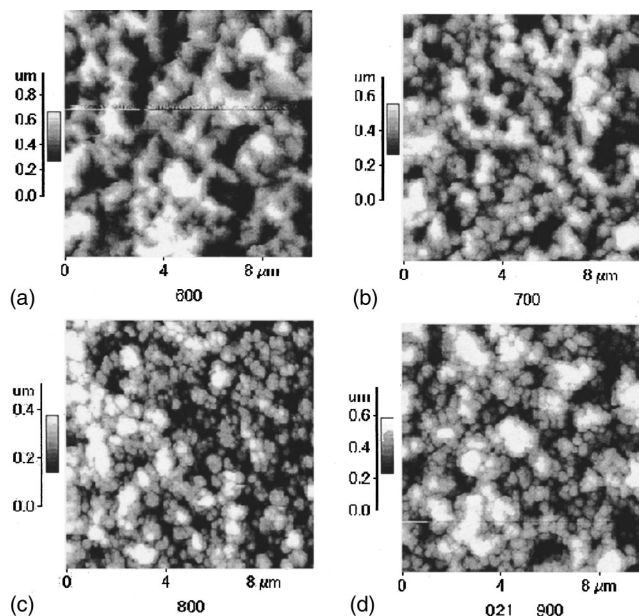


FIG. 2. The pictures of AFM at different annealing temperatures: (a) 600 °C, (b) 700 °C, (c) 800 °C, (d) 900 °C

to transport the reactant, and the total flow rate was kept at 1.3 l/min. The pressure of the growth chamber was 300 Torr. The films were deposited on quartz substrates to be kept at 320 °C. The thickness of the deposited ZnS thin films was about 500 nm. After deposition, thermal oxidation of the films was carried out in oxygen ambient at different temperature range of 500 °C–1000 °C for 2 h. In order to characterize the film structure, x-ray diffraction (XRD) spectra were measured using a D/max-rA XRD spectrometer (Rigaku) with a Cu $K_\alpha$ line of 1.54 Å and atomic force microscopy (AFM) experiment was carried out. Raman and PL spectra were measured using a microlaser Raman spectrometer in a backscattering geometry configuration, a He–Cd laser with a wavelength of 325 nm was used as the excitation source for resonant Raman scattering and PL measurement. The optically pumped lasing experiments were performed using the laser output (320 nm and 200 fs) of an optical parametric amplifier (OPA) in an active passive mode-locked femtosecond Ti–Sapphire laser operating at a repetition rate of 1 kHz. The output of laser was focused on the sample surface with normal incident using a cylindrical lens to form a rectangular stripe of $300\times800\ \mu m^2$. When moving the excitation stripe, a speckled light was observed in high excitation intensity regions. This emission from the edge of the sample was then focused into a monochromator with 0.5 m focal length and detected by a charge coupled device.

## III. RESULTS AND DISCUSSION

### A. Effects of annealing temperature on film structure and morphology

Figure 1 shows the XRD patterns of ZnS thin films annealed at different temperatures from 500 °C to 900 °C. For comparison, the XRD spectrum of an as-deposited ZnS thin film is also given in Fig. 1. The XRD spectrum for an as-deposited ZnS thin film indicates that high-quality ZnS films of a cubic crystal structure have been obtained with a preferred (111) orientation. When the films are annealed at 500 °C, the ZnS begins a transformation to ZnO from a mixed diffraction pattern of ZnS and ZnO in the XRD spectrum. (100), (002), and (101) ZnO diffraction peaks are clearly seen in the XRD spectrum for the sample annealed at 600 °C. We obtain that 52% of ZnS in the thin film transforms to ZnO from the theoretical fitting of all the diffraction peaks in the XRD spectrum. The XRD pattern for the sample annealed at $T_a \geqslant 700$ °C only consists of ZnO diffraction peaks, indicating that the ZnS fully transforms into ZnO with a polycrystalline hexagonal wurtzite structure. From Fig. 1, as the annealing temperature increases, the diffraction peaks of ZnO, such as (101) ZnO peak, become sharper and more intense due to the increased particle size as well as the improved crystallinity. In order to evaluate the mean grain size of the films, the Scherrer's formula[12] is adopted. The mean grain sizes of the films are 20.04, 28.81, 38.41, and 46.10 nm for the samples annealed at 600 °C, 700 °C, 800 °C, and 900 °C, respectively.

For the samples annealed at $T_a \geqslant 700$ °C, only wurtzite ZnO was found in the XRD patterns, indicating the sulfur sites of cubic ZnS were not simply replaced by oxygen during the thermal annealing process. We assume that oxygen atoms diffuse into the ZnS matrix via interstitial sites and bond to Zn, forcing sulfur atoms to occupy the interstitial sites in turn, leading to a modification of the cubic unit network. This way is dominant for the samples annealed at low temperatures.[13] Another way is that oxygen atoms diffuse into the ZnS matrix to occupy the sulfur vacancies induced by thermally fluctuation energy and directly bond to Zn, this way can be dominant at high annealing temperatures. Many point defects, including oxygen vacancies and Zn interstitials, are generated in this process and they assist the unit cell to transform. Because the unit cell of ZnO ($a = 3.249$ Å, and $c = 5.207$ Å) is smaller than that of ZnS ($a = 5.405$ Å), some voids are formed. These will cause the relaxation of the ZnO matrix to a more stable wurtzite structure in accordance with the lowest-energy system. These results indicate that the high-quality nanocrystalline ZnO thin films have been easily obtained by using this method. The pictures of atomic force microscopy (AFM) are shown in Fig. 2, where the thin-film

Downloaded 09 Sep 2012 to 159.226.165.151. Redistribution subject to AIP license or copyright; see http://jap.aip.org/about/rights_and_permissions

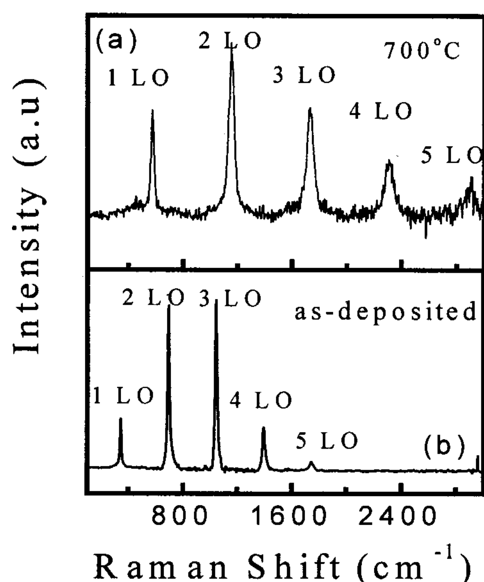


FIG. 3. (a) and (b) represent a typical and RT Raman spectrum of the ZnO films annealed at 700 °C and as-deposited ZnS sample, respectively.

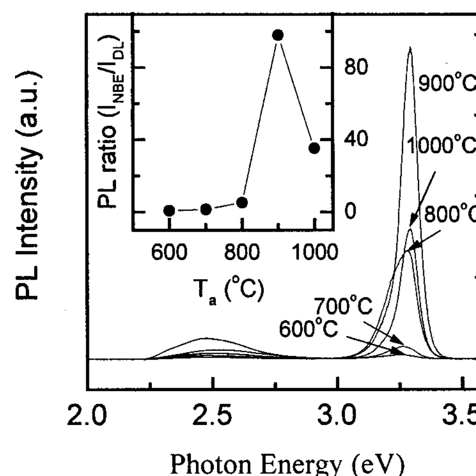


FIG. 4. RT PL spectra of the ZnO thin films at different annealing temperatures, the inset shows the PL intensity ratio of the NBE emission to the DL emission as a function of annealing temperature.

morphology is strongly dependent on annealing temperature. It is important to emphasize that all these samples are from the same cleaved ZnS thin film deposited on a $SiO_2$ substrate. From Fig. 2, the disordered aggregates in the films gradually change into small nanocrystalline balls with a clear interface. The thin films consist of the small nanocrystalline balls with a clear interface as the annealing temperature increases to 900 °C.

## B. Multiple phonon Raman processes

Figure 3(a) shows a typical room temperature (RT) resonant Raman spectrum for the samples annealed at different temperatures ($T_a \geqslant 600\,°C$). For comparison, the Raman spectrum for an as-deposited film is also shown in Fig. 3(b). The Raman spectrum of an as-deposited ZnS thin film is composed of five sharp lines at frequency shifts, which are multiples of the 1-longitudinal optical (LO) zone-center frequency of 343 $cm^{-1}$. Similar frequency shifts are observed for the samples annealed at 500 °C, yet, there was no observation of Raman peak related to ZnO lattice. The Raman spectra for the samples annealed at $T_a \geqslant 600\,°C$ consist of five sharp lines at frequency shifts, which are mu1tiples of the 1-LO ($E_1$) zone-center frequency of ZnO at 581 $cm^{-1}$. Furthermore, it should be noted that Raman scattering peaks of ZnS disappear at the annealing temperature of 700 °C when an $Ar^+$ laser with a wavelength of 488 nm was used as the excitation source (not shown). This result indicates that ZnS has fully transformed into ZnO, which is consistent with the result of the XRD for the sample annealed at 700 °C. In addition, the resonant Raman scattering of the ZnO LO phonon has been observed from Fig. 3(a). The number of multiple phonon-scattering processes observed in semiconductors varies monotonically with the polaron coupling coefficient.[14] ZnO crystal material has large polaron coupling coefficient and large phonon frequency (581 $cm^{-1}$), which results in enormous frequency shifts. Just as $n$(LO) can be compared with $\alpha$, the polaron coefficient, the maximum frequency shift $n(\mathrm{LO}) \times \omega_{\mathrm{LO}}$ can be compared with the deformation energy, which is equal to $1/2\alpha\hbar_{\mathrm{LO}}$. Hence, the large 5-LO Raman frequency shift indicates ZnO has a large deformation energy. To our knowledge, the multiple phonon-scattering processes were observed in ZnO bulk crystal material,[15] but resonant Raman spectra in thin films, so far, have not been reported in literature. A large enhancement in the 2-LO scattered frequency is observed in all the samples annealed at different temperatures, demonstrating a resonant enhancement. The intensity of the $n$-LO ($n > 2$) is also enhanced by the same factor, which is consistent with the theories of multi-LO Raman scattering.[16] The resonant Raman scattering has been previously discussed.[17,18] The results of XRD and Raman scattering indicate that high-quality ZnO films have been obtained.

## C. Photoluminescence

Figure 4 shows the room temperature PL spectra of the ZnS thin films annealed at different temperatures in the range from 600 °C to 1000 °C. The main features of the PL spectra are similar for all samples. The luminescence can be attributed to the NBE emission and the DL emission. The NBE emission around 3.25 eV for the samples annealed at 500 °C has a tendency to blueshift, as compared with the PL of as-deposited samples around 3.12 eV. This result is attributed to ZnO transformed from ZnS with the UV luminescence related to excitons. As the annealing temperature increases from 600 °C to 900 °C, the NBE emission intensity increases remarkably and the peaks become sharper. The NBE emission integrated intensity as a function of annealing temperature is shown in Fig. 5(a). It is similar to that seen in typical bulk ZnO. However, the peak position has a blueshift with the increase of annealing temperature, while a full width at half maximum (FWHM) of the NBE emission decreases gradually. The NBE emission position as well as the FWHM plotted against annealing temperature is shown in Fig. 5(b). The strongest NBE emission with the smallest FWHM of 62 meV is observed around 3.30 eV for the films annealed at

Downloaded 09 Sep 2012 to 159.226.165.151. Redistribution subject to AIP license or copyright; see http://jap.aip.org/about/rights_and_permissions

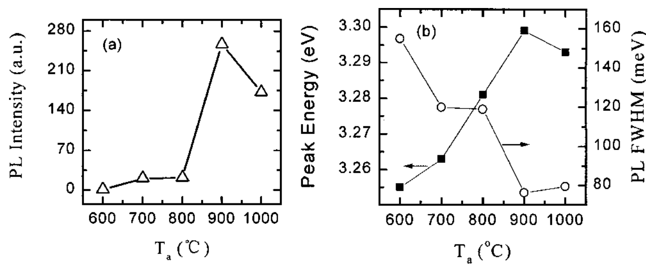


FIG. 5. (a) PL integrated intensity as a function of annealing temperature. (b) PL peak energy position and the FWHM as a function of annealing temperature.

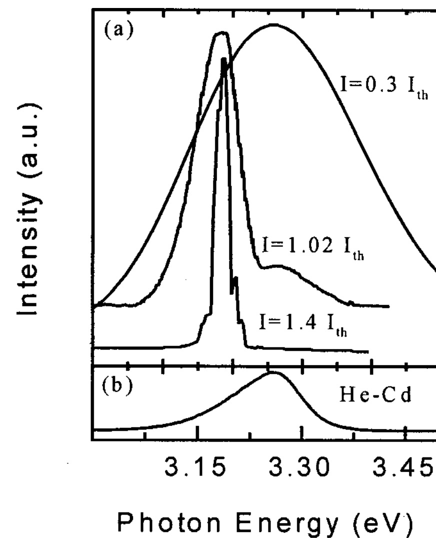


FIG. 6. NBE PL spectra of ZnO thin films annealed at 900 °C. (a) NBE PL spectra at below, near, and above the threshold of 150 kW/cm$^2$, excited by using the laser output (320 nm and pulse width 200 fs) of OPA in an active passive mode-locked femtosecond Ti:Sapphire laser operating at a repetition rate of 1 kHz and (b) PL spectrum excited by the 325 nm line of a He–Cd laser.

900 °C. It is remarkable that the DL emission band around 2.5 eV is barely observable. From XRD patterns and PL spectra, it is confirmed that the film quality is gradually improved as the annealing temperature increases. At a sufficiently high annealing temperature, strain, from the distortion of the ZnO lattice, is eliminated. The defects in the ZnO films are distinctly decreased. It is reasonable to assume that the probability of a bound exciton emission is gradually decreased. The PL peak position shift and the FWHM change are attributed to band structure deformation or lattice deformation.[6] Because the emissions resulted from band structure deformation or lattice deformation are superimposed upon the low-energy side of the NBE emission. This is the reason why upper experimental results are observed. When the annealing temperature is higher than 900 °C, the NBE emission intensity begins to decrease, the FWHM broadens, and the NBE emission peak position becomes redshifted. We explain that, at higher annealing temperature, some new defects, such as oxygen vacancies and Zn interstitials, may be regenerated in ZnO films. Thus, the probabilities of forming a new band structure deformation or lattice deformation increases. This will give rise to a decrease of the NBE emission. Also, the interaction between LO phonon and plasma is enhanced. These mechanisms should result in redshifting and broadening.[19]

One way to evaluate the concentration of structural defects in ZnO films is to compare the PL intensity ratio of the NBE emission to the DL green emission.[6] The reported epitaxial thin films grown by MOCVD[5] and MBE[6] showed relatively weaker DL emissions, with ratios of 1 and 20 at RT, respectively. In the case of bulk material, this ratio usually approached zero as the temperature was increased to 295 K. The best ratio in our experiment is as high as 98 at RT (see the inset in Fig. 4). The FWHM for the samples annealed at 900 °C is as narrow as 62 meV, in comparison with the 117 meV observed for MBE-grown ZnO films at RT. The results of the PL spectra indicate the presence of strong NBE emissions with much weaker DL emissions. The concentrations of the defects responsible for the DL emissions are negligible. On the other hand, when the nanocrystalline sizes are smaller than 55 nm, the films exhibit a strong free- exciton emission with a quantum efficiency that increases with nanocrystalline sizes increasing.[7] These may be the main reason why we can observe the strong NBE emission.

### D. Lasing from thin films

For a comparison of PL line shapes, Fig. 6(a) shows the normalized RT emission spectra from the edge of the nanocrystalline ZnO films at below, near, and above a threshold, $I_{th}$= 150 kW/cm$^2$. As a reference, Fig. 6(b) shows the luminescence spectrum excited by the 325 nm line of a He–Cd laser in a backscattering configuration. An intense NBE emission ($E_{ex}$) is seen at around 3.264 eV.

At low pumping intensities, $I = 0.3\ I_{th}$, a broad emission band is observed at around 3.264 eV with a FWHM of 243 meV. This is the NBE emission. As expected for spontaneous emission, the intensity of this emission band increases linearly with an increase of the pumping intensity below $I_{th}$, 150 kW/cm$^2$. When the ZnO film is pumped at an intensity near the threshold $I_{th}$, $I = 1.02\ I_{th}$, a new and narrow emission peak $p$ emerges directly from the low-energy shoulder of the broad spontaneous spectrum at around 3.178 eV, as shown in Fig. 6(a). At this point emission, the intensity of the $P$ band increases superlinearly with pumping intensity with an unchanged peak position. When the ZnO thin films are excited at $I = 1.4\ I_{th}$, there is a superintense emission peak in the spectrum with a FWHM of 21 meV, as shown in Fig. 7, in contrast to the linear increase in the spontaneous emission intensity. Figure 7 shows the dependence of integrated output intensity on excitation intensity at RT. The linewidth narrowing from 243 to 21 meV, the superlinear increase of the $p$ band intensity as well as the total suppression of the broad spontaneous emission background indicates that stimulated emissions have occurred.[6]

Compared with previous reports on stimulated emissions from ZnO films at RT, the position of our sharp emission peak is found to be in agreement with that expected from an inelastic collision between excitons,[20,21] where one of the two excitons obtains energy from the other and scatters into

Downloaded 09 Sep 2012 to 159.226.165.151. Redistribution subject to AIP license or copyright; see http://jap.aip.org/about/rights_and_permissions

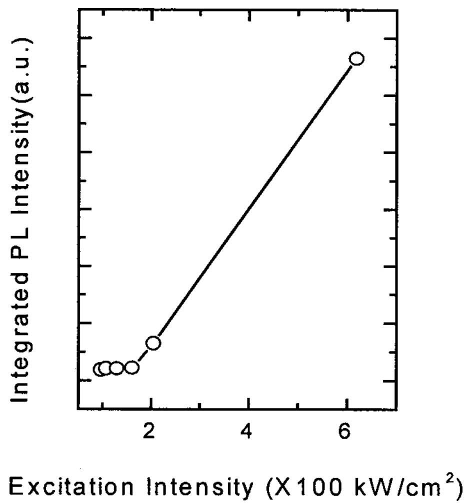


FIG. 7. NBE PL integrated intensity of ZnO thin films annealed at 900 °C as a function of the excitation intensity.

a higher exciton state with a quantum number $n=2$, while the other recombines radiatively. The photons emitted in this process have the energies of $p_n$ given by[20]

$$P_n=E_{ex}-E_b^{ex}(1-1/n^2)-3kT/2 \quad (n=2,3,4,\ldots,\infty), \tag{1}$$

where $p_n$ is the emitted photon energy, $E_{ex}$ is the NBE emission energy, $E_b^{ex}$ is the binding energy of the exciton, $n$ is the quantum number of the envelope function, and $kT$ is the thermal energy. At RT, Eq. (1) gives 84 meV as the energy difference between the NBE emission peak and the exciton–exciton peak. In our experiment, the position of the stimulated emission peak at 3.178 eV is about 86 meV below the NBE emission. This calculated value is in good agreement with our experimental result. Because the peak position of the $p$ band is independent of the pumping intensity, we believe that it also has an excitonic origin.[7]

However, it should be noted that the equally spaced sharp lines of the stimulated emission spectrum are attributed to the multiple longitudinal modes of an optical cavity having a cavity length equal to the entire excitation stripe,[22] indicating the onset of laser action in our nanocrystalline ZnO thin films. Because the line spacing is measured for a Fabry–Pérot resonant cavity with length L, using

$$\Delta E=\frac{\pi ch}{L}\left(n+\frac{Edn}{dE}\right)^{-1}, \tag{2}$$

where $Edn/dE$ is the variation of the refractive index $n$ with photon energy E. The data of the refractive index $n(E)$ are obtained from Ref. 23, and $c$ is light velocity. The good agreement between the calculated values and the measured line spacing between the cavity modes strongly indicates that the sharp lines are due to the longitudinal modes of an optical cavity having a cavity length equal to the entire excitation stripe. The natural optical cavity was formed by the nanocrystalline facets. It is usual for the best cavity modes to be produced from simply prepared samples and the optical cavities are accidentally or naturally formed within the samples. The appearance of the equally spaced sharp lines is from different microlasers in microcavities[21] with different cavity lengths being completely stimulated. A detailed discussion will be published elsewhere.

From an optically pumped lasing experiment, the speckled light around the excitation stripe is observed and no lasing signal is detected except along the direction of the excitation stripe. These results indicate that the planar waveguide decrease light emission scattering. This leads to an increase in optically pumped lasing.

Optically pumped lasing of nanocrystalline ZnO is observed in our experiment at RT. The mean grain size of our films is about 46 nm. When the nanocrystalline size is much larger than the excitonic Bohr radius but smaller than the excitonic coherence length, an excitonic wave function can coherently extend over the nanocrystal. This can lead to a large enhancement in the exciton oscillator strength.[7] The ZnO nanocrystals in our films are spheres with a diameter of about 46 nm. The enhancement factor of the oscillator strength $f$ is expected to be $f/f_{ex}=d^3/\pi^2\alpha_B^3\approx 2\times 10^3$, where $f_{ex}$ is the exciton oscillator strength in bulk crystal and $\alpha_B$ is the exciton Bohr radius ($\alpha_B=1.8$ nm). This huge enhancement of oscillator strength and the effect of the waveguide to limit light scattering may be responsible for the stronger RT optically pumped lasing observed in our samples.

## IV. CONCLUSIONS

We have obtained high-quality nanocrystalline ZnO films with a hexagonal wurtzite structure by thermal oxidation of high-quality ZnS films prepared by the LP-MOCVD technique. A multiple phonon-scattering process in ZnO thin films is observed. When the samples are annealed at 500 °C, ZnS begins to transform into ZnO, and this transformation into ZnO is complete at an annealing temperature of 700 °C. When the annealing temperature increases, the defects in the films gradually decreased and DL emissions become much weaker. The low-energy tail of the NBE emission results from the bound exciton emissions. A strong UV emission is observed at RT for the samples annealed at 900 °C. The PL intensity ratio of NBE emission to DL emission is as high as 98 at RT. We have observed lasing from the high-quality ZnS thin films annealed at 900 °C. This mechanism of laser emission is believed to be exciton–exciton scattering at moderate excitation intensities. It is hoped that devices with much lower thresholds can be produced by further optimizing annealing conditions and improving growth technique.

## ACKNOWLEDGMENTS

The authors would like to thank Dr. J. Judy for her helpful discussions. This work was supported by the Program of CAS Hundred Talents, the National Fundamental Applied Research Project, the Key Project of the National Natural Science Foundation of China No. 69896260, the National Natural Science Foundation of China, the Innovation Foundation of CIOFP, the Excellent Young Teacher Foundation of Ministry of Education of China, and the Jilin Distinguished Young Scholar Program.

Downloaded 09 Sep 2012 to 159.226.165.151. Redistribution subject to AIP license or copyright; see http://jap.aip.org/about/rights_and_permissions

[1] D. A. Gaul and W. S. Rees, Jr., Adv. Mater. **12**, 935 (2000).
[2] M. A. Hasse, J. Qui, J. M. De Puydt, and H. Cheng, Appl. Phys. Lett. **59**, 1272 (1991).
[3] S. Nakamura, M. Senoh, S. Nagahama, N. Iwasa, T. Yamada, T. Matsushita, H. Kiyoku, and Y. Sugimoto, Jpn. J. Appl. Phys., Part 2 **35**, L74 (1996).
[4] L. Stolt, J. Hedström, J. Kessler, M. Ruckh, K. V. Velthaus, and H. W. Schcok, Appl. Phys. Lett. **62**, 597 (1993).
[5] S. Bethke, H. Pan, and B. W. Wesseis, Appl. Phys. Lett. **52**, 138 (1988).
[6] Y. Chen, D. M. Bagnall, H. J. Koh, K. T. Park, K. Hiraga, Z. Zhu, and T. Yao, J. Appl. Phys. **84**, 3912 (1998).
[7] P. Yu, Z. K. Tang, G. K. L. Wong, M. Kawasaki, A. Ohtomo, H. Koinuma, and Y. Segawa, Solid State Commun. **103**, 459 (1997).
[8] R. D. Vispute, V. Talyansky, S. Chooun, R. P. Sharma, T. Venkatesan, M. He, X. Tang, J. B. Halpern, M. G. Spencer, Y. X. Li, G. Salamanca-Riba, A. A. Iliadis, and K. A. Jones, Appl. Phys. Lett. **73**, 348 (1998).
[9] H. Morgan and D. F. Brodie, Can. J. Phys. **60**, 1387 (1982).
[10] D. M. Bagnall, Y. F. Chen, Z. Zhu, T. Yao, S. Koyama, M. Y. Shen, and T. Goto, Appl. Phys. Lett. **70**, 2230 (1997).
[11] Y. Chen, N. T. Tuan, Y. Segawa, H. J. Ko, S. K. Hong, and T. Yao, Appl. Phys. Lett. **78**, 1469 (2001).
[12] B. D. Cullity, *Elements of X-ray Diffractions* (Addison–Wesley, Reading, MA, 1978), p. 102.
[13] Y. Z. Yoo, Y. Osaka, T. Fukumura, Z. Jin, M. Kawasaki, H. Koinuma, T. Chikyow, P. Ahmet, A. Setoguchi, and S. F. Chichibu, Appl. Phys. Lett. **78**, 616 (2001).
[14] J. F. Scott, T. C. Damen, W. T. Silfvast, R. C. C. Leite, and L. F. Cheesman, Opt. Commun. **1**, 397 (1970).
[15] J. F. Scott, Phys. Rev. B **2**, 1209 (1970).
[16] R. H. Callender, S. S. Sussman, M. Selders, and R. K. Chang, Phys. Rev. B **7**, 3788 (1973).
[17] J. F. Scott, R. C. C. Leite, and T. C. Damen, Phys. Rev. **188**, 1285 (1969).
[18] D. C. Hamiton, Phys. Rev. **188**, 1221 (1969).
[19] H. J. Lozykowski and V. K. Shastri, J. Appl. Phys. **69**, 3235 (1991).
[20] C. Klingshirn, Phys. Status Solidi B **71**, 547 (1975).
[21] P. Yu, Z. K. Tang, G. K. L. Wong, M. Kawasaki, A. Ohtomo, H. Koinnuma, and Y. Segawa, Proceedings of the 23rd International Conference on the Physics of Semiconductors, edited by M. Scheffler and R. Zimmermann (World Scientific. Singapore, 1996), p. 1453.
[22] Z. K. Tang, G. K. L. Wong, P. Yu, M. Kawasaki, A. Ohtomo, H. Koinuma, and Y. Segawa, Appl. Phys. Lett. **72**, 3270 (1998).
[23] W. L. Bond, J. Appl. Phys. **36**, 1674 (1965).

Downloaded 09 Sep 2012 to 159.226.165.151. Redistribution subject to AIP license or copyright; see http://jap.aip.org/about/rights_and_permissions